Microporous and Mesoporous Materials 346 (2022) 112308

Contents lists available at ScienceDirect

Microporous and Mesoporous Materials

journal homepage: www.elsevier.com/locate/micromeso

Stepwise dehydration of thomsonite (THO) with disordered Si/Al distribution: A new partially hydrated phase

Matteo Giordani [a], Katarzyna Skrzyńska [b], Georgia Cametti [c,*]

[a] Department of Pure and Applied Sciences, University of Urbino Carlo Bo, 61029, Urbino, Italy
[b] Institute of Earth Sciences, Faculty of Natural Sciences, University of Silesia, Będzińska 60, 41-200, Sosnowiec, Poland
[c] Institute of Geological Sciences, University of Bern, Baltzerstrasse 1+3, 3012, Bern, Switzerland

ARTICLE INFO

Keywords:
Zeolites
Dehydration
THO
XRD

ABSTRACT

The structural transformations occurring as a function of increasing temperature in zeolites are of interest because the porous structure, and therefore the physical properties, can significantly change.

Zeolites with **THO** framework type are small-pore materials, which received attention because of their applications in catalytic processes. The majority of **THO** zeolites (synthetic and natural) are characterized by an ordered distribution of the cations at the tetrahedral sites. To date, few cases of disordered thomsonite have been reported. In this study, we investigated the dehydration behaviour of a natural thomsonite with disordered Si/Al distribution and chemical composition $Ca_{3.34}Na_{2.66}Si_{11}Al_9O_{40}\bullet 12H_2O$. The structure was determined from room temperature (RT) to 698 K in order to compare the thermal behaviour with that reported for the ordered variety. Accurate structural analysis was performed by *in situ* single crystal X-ray diffraction. The dehydration starts at 348 K. Up to 498 K, thomsonite gradually releases four H_2O. From 498 to 573 K, additional four H_2O are lost and the space group changes from orthorhombic (*Pbmn*) to monoclinic ($P2_1/n$). This partially hydrated phase is characterized by a unit-cell volume contraction of −3% with respect to the RT phase and by a rearrangement of the extraframework cations in the zeolitic pores. The thermally treated thomsonite is able to reabsorb 50% of the lost H_2O and transforms to the orthorhombic phase, equivalent to that observed at lower temperatures. However, the diffraction pattern analysis indicated a high degree of mosaicity, most probably due to the residual stress accumulated during the phase transformation.

1. Introduction

Zeolites with **THO** framework type have pores size between 2 and 4 Å and openings limited to 8-membered rings (8mr) of tetrahedra [1]. They are therefore classified as small-pores materials. The topological symmetry of thomsonite is orthorhombic, space group *Pmma* (#51), with idealized cell parameters a = 14.0, b = 7.0, c = 6.5 Å. Because of Si/Al ordering at tetrahedral sites and extraframework (EF) cations distribution, the actual reference material, with chemical composition $Na_4Ca_8Al_{20}Si_{20}O_{40}\bullet 24H_2O$, is described in the orthorhombic space group *Pncn* (#52), with cell parameters a = 13.088, b = 13.052, c = 13.229 Å [1–3]. The framework consists of cross-linked T_5O_{10} chains, also referred as 4-1 Secondary Building Units (SBU), running parallel to the *c*-axis. These building units are characteristic of the so-called "fibrous zeolites group" [1,4,5], which includes zeolites with **EDI**, **NAT**, and **THO** framework types. The different connectivity pattern of the T_5O_{10} chains originates different framework topologies. In **THO**, the 8mr channels run along [100] and [001]. These channels host Ca, Na, and H_2O in the natural samples. Synthetic analogues of thomsonite with a variety of chemical elements at the tetrahedral sites (i.e. zinc-phosphates, aluminium-cobalt-phosphates, gallium-germanium, etc.) were also produced [6–10].

The structure of thomsonite was at first reported [11] in space group *Pbmn* (#62) with a = 13.0, b = 13.05, and c = 6.6 Å, i.e. with half c-parameter with respect to the reference material. Later, Amirov et al. [12] also described a thomsonite with c = 6.6 Å, but in this case, the structure was solved in the space group *Pncn*. Furthermore, the authors pointed out a disordered Si/Al distribution at the tetrahedral sites. Similarly, Gatta et al. [13] found a sample of disordered thomsonite (*Pbmn*) with c = 6.60 Å. A set of measurements were performed in the range from 98 to 297 K, but no significant changes were observed as a function of temperature. Nevertheless, the disordered variety of

* Corresponding author.
E-mail address: georgia.cametti@geo.unibe.ch (G. Cametti).

https://doi.org/10.1016/j.micromeso.2022.112308
Received 30 September 2022; Accepted 20 October 2022
Available online 25 October 2022

thomsonite is rare and the majority of **THO** materials (both natural [2–4, 14] and synthetic [6–10]) are characterized by an ordered distribution of the tetrahedral cations at the T sites and by a c-parameter ~ 13.2 Å.

The dehydration behaviour and thermal stability of ordered thomsonite were investigated by X-ray powder diffraction and thermogravimetric analysis [15,16] up to 573 K. The changes observed as a function of increasing temperature consisted in the release of the H_2O from one of the four H_2O sites and a decrease in the unit-cell volume. The orthorhombic space group was maintained up to 573 K, although "a major structural change" was reported [16], the nature of which remained unsolved. At higher temperatures, thomsonite turned amorphous.

In this study, we investigated the dehydration of a thomsonite with a disordered Si/Al distribution and half c-parameter with respect to the reference material. The aim was to determine: i) the structure of the high-temperature phase; ii) its eventual rehydration capacity, and iii) whether the thermal behaviour of disordered thomsonite was similar to that of the ordered variety. To perform an accurate structural analysis, we monitor *in situ* the structural modifications by single-crystal X-ray diffraction. With this approach, we could identify a phase transition, which accompanies the dehydration process and leads to a new partially-hydrated monoclinic structure, which is possibly stable until the structural collapse.

2. Methods

The sample consisted of a natural thomsonite taken from the specimen investigated by Giordani et al. [17]. The chemical composition was $Ca_{3.34}Na_{2.66}Si_{11}Al_9O_{40}\bullet 12H_2O$.

The data were collected on a crystal with dimension 0.250 × 0.200 × 0.06 mm using a Synergy-S single crystal X-ray diffractometer equipped with a double microfocus source and a HyPix-6000HE detector. At first, new data were collected at room temperature using the AgKα (λ = 0.56087 Å), ensuring I/σ(I) = 30. Data were processed and reduced by the software CrysAlisPro 171.42.58a [18]. The indexing of the reflections indicated an orthorhombic unit-cell with dimension a = 13.0515(5), b = 6.5999(2), c = 13.0930(5) Å, and V = 1127.82(7) $Å^3$. An inspection of the reciprocal space did not point out any reflection with significant intensity at b*/2. The structure was solved by direct methods [19] in the space group *Pmna* transformed to *Pbmn* (unit-cell: a = 13.0930(3), b = 13.0515(5), c = 6.5999(2) Å, V = 1127.81(7) $Å^3$) for a better comparison with literature data [13]. Structural refinements were performed using neutral atomic scattering curves with the software Shelxl-2014 [20].

The high-temperature (HT) measurements were performed using an Oxford Cyberstar nitrogen blower, mounted on the same diffractometer. The data were collected *in situ,* and the temperature was increased from 298 to 698 K in steps of 75 K. Before the data collection, the crystal was equilibrated at a given temperature for at least 40 min. These experimental conditions can be regarded as dry conditions.

From 348 to 498 K, the structure solution indicated the space group *Pmna*. At 573 and 648 K, the structure was solved and refined in the monoclinic space group $P2_1/n$. Additional tests were performed in the space group *Pmmn*, but this solution was discarded because of the poor quality of the refinement. The structure was refined as a two-component twin, with TWIN law [-100 010 00–1] and BASF parameter equal to 0.337(4). After heating at 698 K, a screening of the crystal revealed only a few extremely weak broad reflections. Therefore the experiment was stopped. We did not further increase the temperature in order to avoid structural collapse and to proceed with the investigation of the rehydration capacity.

After the HT measurements, the same crystal was exposed to high-humidity conditions (relative humidity >80%) in order to check if rehydration occurred. A new data set was collected at ambient conditions after 13, 30, and 56 days of exposure, with the same diffractometer used for the temperature-dependent measurements. However, due to the weak scattering power of the crystal, the CuKα radiation (λ = 1.54184 Å) was used.

Data collection and refinements parameters are reported in Table 1. All structural drawings were produced by the software VESTA [21]. Crystallographic information files (Cifs) of the structure measured a RT, 498, 573 K and at RT after the rehydration experiments (sample THO_Rehy56) have been deposited as supplementary materials.

3. Results

3.1. The room temperature structure

Diffraction data obtained at RT clearly indicated that the thomsonite sample investigated in this study has a half c-parameter (Table 1) with respect to the reference material thomsonite [1] and its synthetic counterparts [6–10]. The structure refinement in space group *Pbmn* indicated a disordered Si/Al distribution (Table 2), in agreement with previous findings, which showed that the ordering of Si/Al at the tetrahedral sites is observed only for thomsonite with c ≈ 13 Å. The extraframework cations, Na and Ca, are distributed over two sites, Na and Ca. The first one is fully occupied by 33% of Ca and 66% of Na, whereas the Ca site is off from the mirror plane perpendicular to the b-axis, and it is therefore split in two equivalent positions (Table S1). The H_2O fully occupies the W1, W2, and W3 sites. This configuration resembles that reported by Gatta et al. [13] for a disordered thomsonite with cell parameters similar to those obtained in our study. An inspection of the difference Fourier maps allowed the localization of the corresponding hydrogen atoms, H1, H2, and H3, and the analysis of the hydrogen bonds (Table 3). The W1–H1···O6 and W3–H3···O6 interactions are fairly strong with H···O acceptor distance of 1.91(2) and 1.92(3) Å, respectively, although the unfavourable DHA angle (151(2) and 145(3)°) compared to the W2–H2···O5 (DHA = 167(3)). This geometrical configuration agrees with that determined at 295 K by Gatta et al. [13].

3.2. Structural modifications upon heating

The evolution of the unit-cell volume of thomsonite and the corresponding H_2O content as a function of temperature is reported in Fig. 1. The dehydration starts at 348 K when the structure loses $0.5H_2O$. No significant modifications are observed up to 573 K. In this temperature range, the structure gradually releases water. In particular, the site occupancy factor (*sof*) of the W3 site decreases from 1 (at RT) to 0.159(13) at 498 K (Table S2). The water loss does not affect the positions of the EF cations, which remain unaltered.

At 573 K, the pronounced decrease of the unit-cell volume (-3% with respect the one measured at RT) is accompanied by a phase transformation from orthorhombic *Pbmn* to monoclinic space group $P2_1/n$. This change involves doubling the c-parameter, from 6.6274(2) to 12.8281(4) Å, the further release of $4H_2O$, and a rearrangement of the EF cations in the structural voids. In the investigated temperature range, the structure does not dehydrate completely. Approximately 33% of the initial water content is retained up to 648 K. No significant differences were found between the structure measured at 573 and 648 K, with the exception of a slight decrease of the W2 occupancy from 1 to 0.95(2). Hereafter, we discuss the high-temperature modification based on the 573 K data set.

3.2.1. The high-temperature phase

The framework of the high-temperature (HT) phase is characterized by a rotation of the tetrahedra constituting the 4-1 SBU and consequent deformation of the 8mr channels parallel to [010] with respect to the RT phase (Fig. 2a and b). This deformation can be interpreted as a deviation from 180° of the T3-T3-T3 angle (α) measured along the c-axis (Fig. 2a and b). In the RT phase, α is equal to 180°, being the T3 sites of the 4-1 SBU aligned along the c-axis. At high temperatures, the angle decreases to 167.5° as a consequence of the monoclinic distortion.

Table 1
Crystal data and refinement parameters of disordered thomsonite at RT, 498, 573 K, and after 56 days of exposure to high humidity conditions.

Crystal data	THO_RT	THO 498 K	THO 573 K	THO_Rehy56
a (Å)	13.0930(5)	13.0355(4)	12.9947(4)	12.9625(7)
b (Å)	13.0515(5)	13.0109(4)	13.2016(5)	12.9465(9)
c (Å)	6.5999(2)	6.6274(2)	12.8281(4)	6.6007(4)
γ (°)			90.141(3)	
V (Å^3)	1127.81(7)	1124.03(6)	2200.66(13)	1107.72(12)
Z	1	1	2	1
Space Group	*Pbmn*	*Pbmn*	$P112_1/n$	*Pbmn*
Refined Chemical formula	$Ca_{3.34}Na_{2.66}(Al,Si)_{20}O_{40}$ •$12H_2O$	$Ca_{3.28}Na_{2.73}(Al,Si)_{20}O_{40}$ •$8.6H_2O$	$Ca_{3.35}Na_{2.75}(Al,Si)_{20}O_{40}$ •$4H_2O$	$Ca_{2.95}Na_{2.99}(Al,Si)_{20}O_{40}$ •$7.7H_2O$
Crystal size (mm)	0.250 × 0.200 × 0.06	0.250 × 0.200 × 0.06	0.250 × 0.200 × 0.06	0.250 × 0.200 × 0.06
Data collection				
Diffractometer	XtaLAB Synergy, Dualflex, Hypix	XtaLAB Synergy, Dualflex, Hypix	XtaLAB Synergy, Dualflex, Hypix	XtaLAB Synergy, Dualflex, Hypix
X-ray radiation	Ag $K\alpha$, $\lambda = 0.56087$ Å	Ag $K\alpha$, $\lambda = 0.56087$ Å	Ag $K\alpha$, $\lambda = 0.56087$ Å	Cu $K\alpha$, $\lambda = 1.54184$ Å
Temperature (K)	293	498	573	293
Exposure time (s)				
Max. 2θ (°)	49.84	49.86	50.17	152.72
Index ranges	$-19 \le h \le 18$ $-16 \le k \le 14$ $-8 \le l \le 9$	$-19 \le h \le 19$ $-17 \le k \le 18$ $-9 \le l \le 9$	$-19 \le h \le 19$ $-19 \le k \le 17$ $-16 \le l \le 18$	$-16 \le h \le 16$ $-16 \le k \le 14$ $-8 \le l \le 4$
No. of measured reflections	8018	21178	29249	4457
No. of unique reflections	1641	1859	6494	1170
No. of observed reflections $I > 2\sigma$ (I)	1484	1652	5500	946
Structure refinement				
No. of parameters used in the refinement	109 + 3 restraints	102	310	102
R(int)	0.0281	0.0393	0.1007	0.0478
R(σ)	0.0226	0.0205	0.0634	0.0277
GooF	1.062	1.082	1.076	1.201
$R1$, $I > 2\sigma$ (I)	0.0320	0.0311	0.0841	0.1035
$R1$, all data	0.0352	0.0354	0.0964	0.1208
w$R2$ (on F^2)	0.0993	0.1025	0.2048	0.2949
$\Delta\rho_{min}$ (-eÅ^{-3}) close to	−0.80 NaB	−0.60 NaB	−1.00 T2MA	−0.55 T2
$\Delta\rho_{max}$ (eÅ^{-3}) close to	0.64 W1	0.70 NaB	0.94 Na1A	0.90 T2

Table 2
Relevant T-O distances (in Å) of disordered thomsonite at RT. The average distance (<T-O>) for each tetrahedral site is also reported.

T1-O1	1.6741(8)	T2-O6	1.6725(13)
T1-O5	1.6747(14)	T2-O4	1.6814(14)
T1-O2	1.6770(14)	T2-O2	1.6841(15)
T1-O4	1.6831(14)	T2-O3	1.6889(10)
<T-O>	1.677		1.682

In the HT modification, because of the deformation and lowering of symmetry, there are two channels (Ia and Ib) independent for symmetry running parallel to the b-axis (Fig. 2b). Compared to the RT structure, one channel (Ia) is more elliptical whereas the other (Ib) has a more roundish shape (Table 4). The 8mr channels parallel to [001] (Fig. 2c and d) are also affected by such rotation, as demonstrated by the change in the size of the apertures (O–O distances in Table 4).

The residual water in the structure measured at 573 K distributes over two fully occupied sites, W1M and W2M (Table S3). It should be noticed that these sites are not equivalent to W1 and W2 of the orthorhombic phase. Indeed, the unit-cell of the orthorhombic phase hosts $4H_2O$ at each W site. At first, with the increase of temperature (up to 498 K) $4H_2O$ are released from the W3 site. In concomitance of the phase transformation, the structure releases additional $4H_2O$, most probably from the W2 sites. Therefore, W1 and W2 must not be considered equivalent to W1M and W2M.

At 573 K, the EF cations rearrange in the structural voids as follows:

- Na atoms, which in the RT structure are found in the middle of channel IIb, coordinating four H_2O (two at W3 and two at W1 sites), and four oxygen atoms (two at O2 and two at O3), seem to maintain their original positions, though split in two sub-sites (Na1 and Na1A) (Fig. 3a and b). They form bonds with two H_2O at W1M and three oxygen atoms at O4, O4MB, O5MA, and O1.
- Ca is at a fully occupied site (Ca1) in the middle of IIa channel (Fig. 3b), where it bonds to two H_2O at W2M and four oxygen atoms at O3, O3M, O2MA, and O2. Additional Ca distributes over Ca2, Ca22, and Ca23 sites, which on average coordinates only to framework oxygen atoms (O5MB, O5M, O6, O6M). This might correspond to the Ca at the Na site in the low-temperature modification that, after the loss of H_2O, moves in the middle of the 8mr channels parallel to the b-axis (channel Ib), closer to the framework oxygen atoms.

3.3. The rehydrated structure

The rehydration capacity of thomsonite was checked after 13 (THO_Rehy13), 30 (THO_Rehy30), and 56 (THO_Rehy56) days by exposing the thermally treated sample to high humidity conditions (RH > 80%).

Table 3
Hydrogen bond-net of disordered thomsonite at RT. Donor-hydrogen (DH), hydrogen-acceptor distances (HA), and donor-hydrogen-acceptor angles are reported for each water molecule.

D	H	A	DH(Å)	HA(Å)	DA(Å)	DHA(°)
W2	H2	O5	0.89(2)	1.99(2)	2.867(2)	167(3)
W1	H1	O6	0.89(2)	1.91(2)	2.7269(17)	151(2)
W3	H3	O6	1.01(2)	1.92(3)	2.8102(15)	145(3)

D = donor.
H = hydrogen.
A = acceptor.

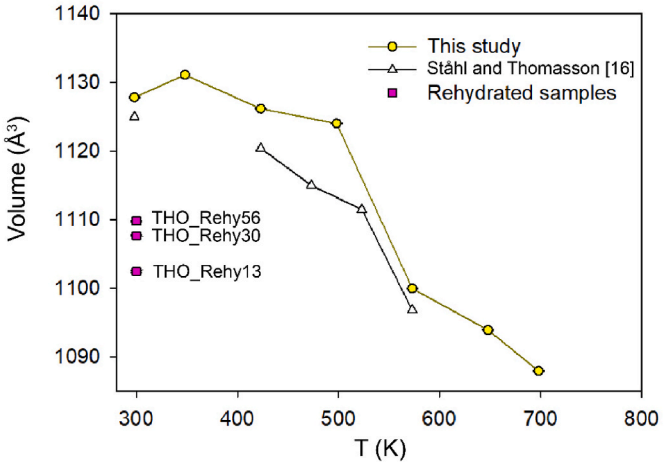

Fig. 1. Unit-cell volume trend of thomsonite as a function of temperature. The data from this study (disordered thomsonite) and those from Ståhl and Thomasson [16] (ordered thomsonite) are displayed as circles and triangles, respectively. The corresponding values of the rehydrated samples after different exposure times (13, 30, and 56 days) to high humidity conditions are shown with square symbols.

No significant differences, with the exception of a slight unit-cell volume increase in THO_Rehy56, were noticed among these partially rehydrated structures. Overall, after 13 days, thomsonite was able to reabsorb approximately 50% of the lost H_2O. The prolongation of the exposure time to additional 43 days did not bring to any improvement, neither in terms of quality of the crystal structure nor of amount of H_2O content. Hereafter, we discuss the results of the THO_Rehy56 (Table S4).

The diffraction pattern of the THO_Rehy56 structure was characterized by broad and weak reflections, the intensity of which significantly decreased at d < 1.0 Å. The indexing of the reflections indicated a unit-cell with a c-parameter = 6.60 Å (Table 1), although weak reflections were detected along ½ of the c* axis. Data reduction and subsequent structure solution pointed to the orthorhombic space group *Pmna*, equivalent to the RT phase.

Test refinements were also performed in the monoclinic space group *P2/n*. In both crystal systems, forbidden reflections and inconsistent equivalents were detected. Furthermore, lowering the symmetry did not bring significant improvement; therefore, the *Pmna* space group was maintained. The diffraction patterns quality and the data reduction results indicated that this partially rehydrated structure can be interpreted as an intermediate modification between the orthorhombic and monoclinic phase. The presence of very weak reflections at ½ c* axis further supports this hypothesis. Despite this, the structure, in terms of framework and EF cations distribution, is close to that measured at RT. The monoclinic distortion observed at 573 K is no longer present, i.e. the tetrahedra forming the SBU are aligned along the c-axis with corresponding α angle = 180°. The refined water content amounts to $8H_2O$ pfu, indicating that thomsonite, under these experimental conditions, could reabsorb half of the lost H_2O. The Na and Ca atoms relocate and occupy EF sites corresponding to those of the RT phase (Fig. 3c). Similarly, the reabsorbed H_2O resides at W1 and W2 sites (Table S4).

4. Discussion

4.1. The partially dehydrated phase: comparison with ordered thomsonite

Our data at room temperature clearly indicate that the investigated thomsonite has half the c-axis and a disordered Si/Al distribution. According to literature data, including the X-ray powder diffraction characterization of the specimen used in our study [17], the disordered thomsonite is rarer than the ordered one. However, both varieties can

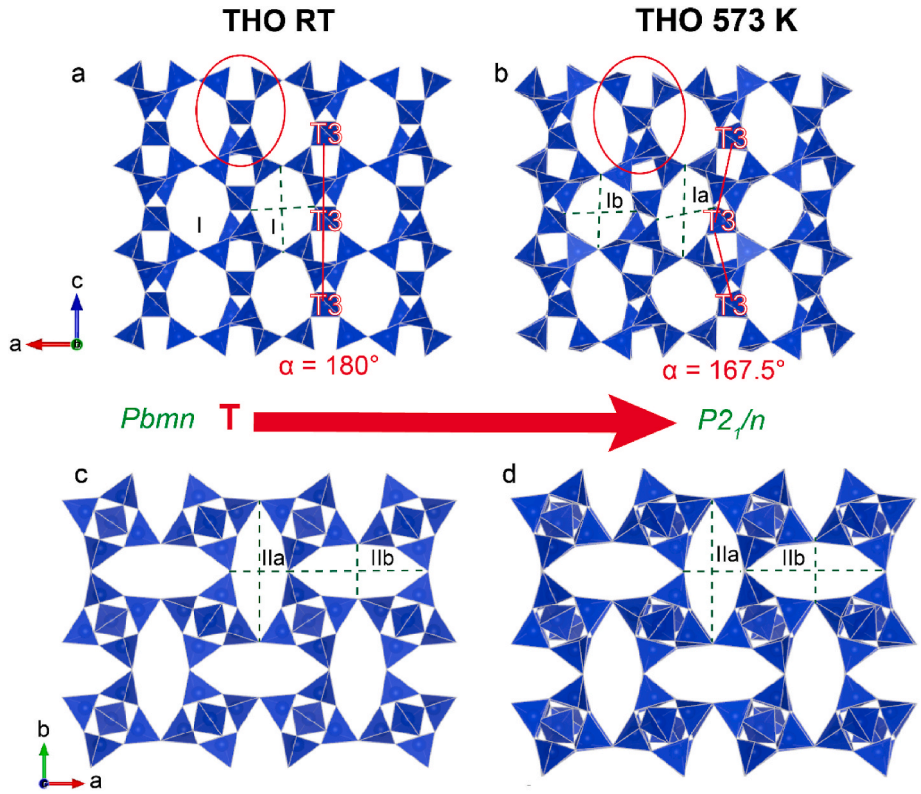

Fig. 2. Polyhedral representation of the crystal structure of disordered thomsonite at RT (a,c) and at 573 K (b,d) projected along b and c-axis, respectively. The EF occupants are omitted for the sake of clarity. The red circles highlighted the 4-1 SBU. The T3-T3-T3 angle (α) is reported for the two phases. (For interpretation of the references to color in this figure legend, the reader is referred to the Web version of this article.)

Table 4
Free diameters (in Å) of the eight-membered ring (8mr) channels parallel to [010] and [001] in disordered thomsonite at RT and 573 K. The given values are obtained by subtracting to the O–O distances twice the oxygen radius of 1.5 Å [1].

	RT		573 K	
8mr [010]	Channel I		Channel Ia	
	O3–O3	3.90	O3–O3M	4.39
	O5–O5	2.25	O5M-O5MB	1.80
			Channel Ib	
			O3–O3M	3.04
			O5–O5MA	2.79
8mr [001]				
Channel IIa	O3–O3	6.73	O3–O3M	6.69
	O1–O1	2.17	O1–O1M	2.17
Channel IIb	O1–O1	7.09	O1M-O1	6.88
	O3–O3	0.93	O3–O3M	1.11

coexist in the same specimen. According to the chemical composition of our sample ($Ca_{3.34}Na_{2.66}Si_{11}Al_9O_{40}\bullet 12H_2O$) and that investigated by Gatta et al. [13] ($K_{0.01}Na_{2.11}Ca_{2.92}Mg_{0.25}Al_{8.4}Si_{11.56}O40\bullet 11.8H_2O$, also with a disordered Si/Al distribution at the T sites), the disordered thomsonite seems to be Ca-poor with respect to the ordered one [2–4, 14]. We suggest that in natural samples the substitution mechanism $Na^{+} + Si^{4+} \rightarrow Ca^{2+} + Al^{3+}$ may take place in crystallization environment locally enriched in Si and Na. This could be the cause of the locally observed Si/Al disorder. Interestingly, among the synthesized zeolites with **THO** framework type, a structure with disordered cation distribution at the tetrahedral sites and half c-axis was never reported [6–10].

The dehydration behaviour of disordered thomsonite can be summarized as a transformation from orthorhombic to monoclinic between 498 and 573 K, accompanied by a decrease of the unit-cell volume ($\Delta V = -3\%$) with respect that measured at room temperature. The transformation from *Pbmn* to $P2_1/n$ is triggered by the water release, which is a gradual process, though the release of $4H_2O$ between 498 and 574 K seems to be more abrupt. In the investigated temperature range,

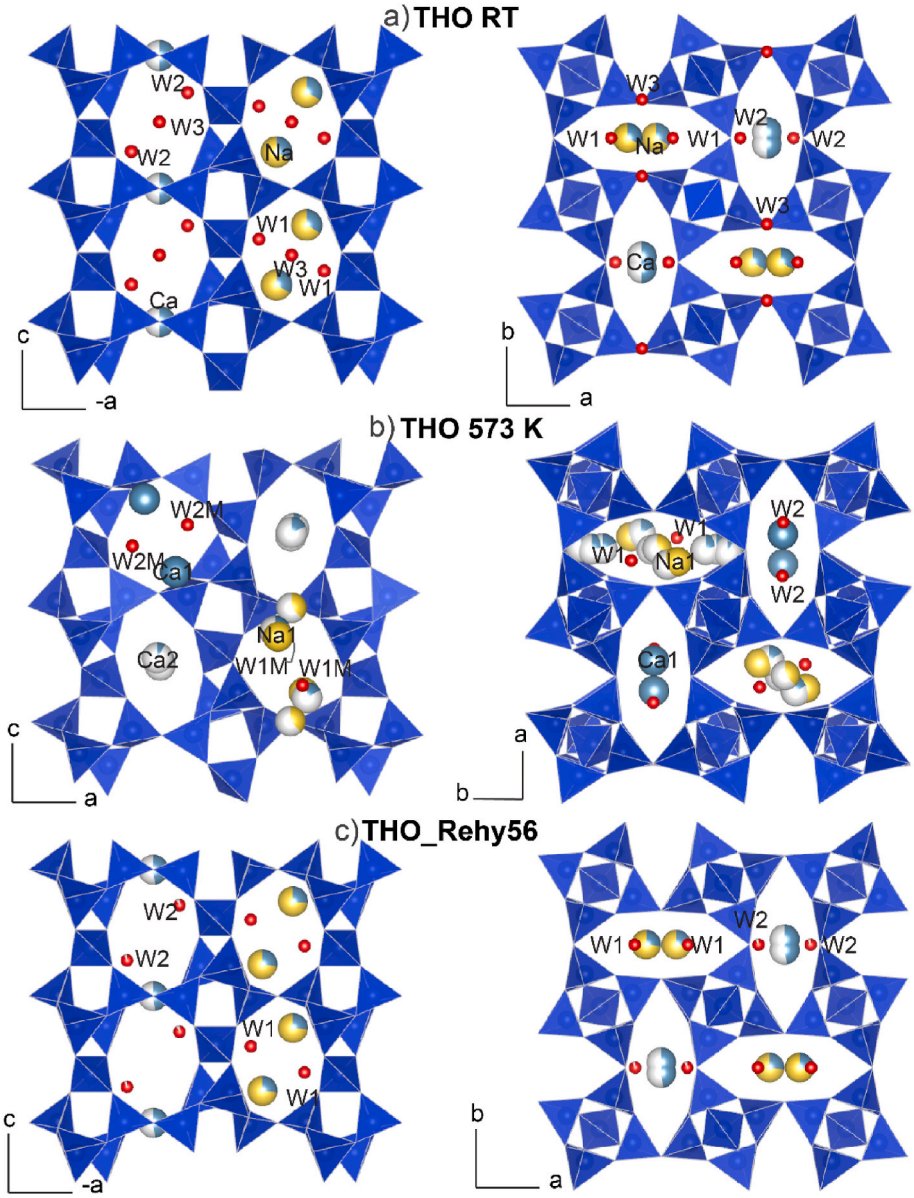

Fig. 3. Crystal structure of disordered thomsonite projected along b- and c-axis at RT (a), 573 K (b), and after rehydration (sample THO_Rehy56) (c). Ca, Na, and O of the H_2O molecules are represented as dark cyan, yellow, and red spheres, respectively. Partially colored spheres correspond to partially occupied sites. Hydrogen atoms in the RT structure are not shown. (For interpretation of the references to color in this figure legend, the reader is referred to the Web version of this article.)

thomsonite does not dehydrate completely. The diffraction pattern collected at 648 K suggests that the structure is close to structural collapse, but it partially retains water molecules. The trend of the unit-cell volume as a function of temperature is similar to that calculated from the data by Ståhl and Thomasson [16] (Fig. 1). This is not surprising because of the extended data collection time (12 h) that can be regarded as close to equilibrium conditions, similar to our experimental set-up. Moreover, the H_2O are released from the same crystallographic positions (W3 and W4 in Ref. [16] are equivalent to the W3 site in our structure). The H_2O at W3 is the one less strongly bonded to EF cations; therefore, it is plausible that it is the first to be released.

Our findings are very similar to those reported by Reeuwijk [15] for a natural sample of ordered thomsonite. The author reported the loss of $8H_2O$ in the temperature range between 273 and 473 K, accompanied by the contraction of the a-axis and a minor expansion along the c-axis. In the next heating steps, between 598 and 623 K, additional H_2O was released and a "distinct metaphase" formed. At 663 K, the transition to a phase with very weak reflections was reported, the rehydration of which was not possible. Further, although the lattice was destroyed already at 723 K, nearly $2H_2O$ were lost only at higher temperatures [4]. Similarly, Ståhl and Thomasson [16] stated that a "major structural change" at 573 K, associated with a decrease in the site occupancy of the EF cations, could not be "fully understood". Based on our results, we hypothesize that the structural changes in ordered thomsonite, in terms of adjustment of the tetrahedral framework and diffusion of the EF cations, might be similar to those observed in the disordered thomsonite and, possibly, the space group might change.

It should be pointed out, that among the synthetic materials with **THO** framework type, a monoclinic phase with space group $P2_1/n$ was reported for two zeolites, a gallium-cobalt-phosphate (sample GCP-THO4 in Ref. [6]) and a zinc-aluminum-arsenate (ZnAlAs-THO [10]). Nevertheless, these structures are not equivalent to our partially dehydrated disordered thomsonite. The unit-cell volume and the channel sizes are significantly larger than in the high-temperature phase observed in our study, resulting in a different channel configuration [10].

4.2. Reabsorption of structural water: comparison with other fibrous zeolites

The rehydration experiments indicated that thomsonite, after 13 days of exposure to ambient temperature and high humidity conditions, partially reabsorbs H_2O. However, the amount of the reabsorbed H_2O does not increase after prolonged exposure time (up to 56 days), suggesting that complete rehydration is extremely slow or eventually not achievable under these conditions. Hence, the structure is able to uptake $4H_2O$ in a relatively short timeframe, but subsequently, it reaches a steady state. The observed rehydration behaviour leads to a phase, which is not equivalent to that measured at RT, but resembles the configuration observed between 498 and 573 K. The diffraction pattern (presence of forbidden reflections, low-intensity reflections) reveals that this structural configuration might be a relic of the distorted phase observed at HT.

This "strain-induced mosaicity resulting from the phase transition" [22] was also observed in other fibrous zeolites upon rehydration, i.e. natrolite [22,23], mesolite [24], and scolecite [25]. In particular, the experimental procedure to test the dehydration and rehydration capacity of scolecite [25] was equivalent to that applied in this study, making a comparison between the two more significant. In contrast to thomsonite, despite the structural strain, both scolecite and natrolite are able to reabsorb all water lost during the dehydration process.

On a general scale, the parallelism between the high-pressure and high thermal behaviour of fibrous zeolites is worth mentioning. The rotation of the SBUs observed upon heating is equivalent to the distortion mechanism observed under increasing pressure [26–28], which brings to the contraction of the unit-cell volume.

Concerning the limited (or sluggish) rehydration capacity, we provide here a possible interpretation. Thomsonite maintains the orthorhombic space group if the structure contains approximately $8H_2O$ per formula unit. The release of extra $4H_2O$ occurs in a short temperature range, i.e. between 498 and 573 K. As soon as the structure releases this amount of water (located at the W2 site), the coordination environment becomes unfavourable for Ca atoms, and the structure changes to the monoclinic phase. Similarly, the re-uptake of $4H_2O$ during the rehydration experiments seems to be relatively fast, whereas the reabsorption of water, located at the W3 site in the RT structure, is sluggish or maybe not achievable. The reabsorption of additional water might be hampered by the residual stress accumulated during the phase transformation. However, it does not seem to be the case since the system of channels of THO_Rehy56 structure, although slightly contracted (1.5%), is equivalent to that of the RT structure. Alternatively, water reabsorption at W3 might not be indispensable to stabilize the structure. Indeed, according to bond-valence calculations, the values obtained for both Ca and Na are close to the ideal bond-valence sum (Table S5).

5. Conclusions

In this study, we investigated the dehydration and rehydration behaviour of a thomsonite zeolite with disordered Si/Al distribution at the tetrahedral sites. The dehydration was followed stepwise, and the results showed a main structural change occurring between 498 and 573 K. Overall, the observed changes can be summarized as follows: i) release of 50% of the structural water; ii) transformation from orthorhombic *Pbmn* to monoclinic $P2_1/n$; iii) migration and rearrangement of the EF cations (Na and Ca) in the structural voids. The partially hydrated monoclinic phase was determined for the first time. In the investigated temperature range, the structure does not dehydrate completely, and after exposure to high humidity conditions, it is able to reabsorb 50% of the lost water molecules. The rehydrated structure is equivalent (in terms of space group and topology) to the RT one. However, the diffraction pattern highlighted residual stress, most probably due to the experienced phase transformation. The same "stress-induced mosaicity" [23] was also reported for other fibrous zeolites.

Previous studies reported on the high-temperature modification of ordered thomsonite, the structure of which remained unsolved. Based on our results, we suggest that the extent of structural transformations and the structural rearrangements for ordered thomsonite might be very similar to those observed in our study.

CRediT authorship contribution statement

Matteo Giordani: Conceptualization, Methodology, Writing – review & editing. **Katarzyna Skrzyńska:** Formal analysis, Investigation, Writing – review & editing. **Georgia Cametti:** Conceptualization, Formal analysis, Investigation, Methodology, Supervision, Writing – original draft.

Declaration of competing interest

The authors declare that they have no known competing financial interests or personal relationships that could have appeared to influence the work reported in this paper.

Data availability

The data have been provided as Supplementary Material

Acknowledgments

Funding The National Science Center of Poland is acknowledge by K. S. [grant number UMO-2019/35/O/ST10/01015]; Preludium Bis 1 project of the Polish National Agency for Academic Exchange.

Appendix A. Supplementary data

Supplementary data to this article can be found online at https://doi.org/10.1016/j.micromeso.2022.112308.

References

[1] C. Baerlocher, W.M. Meier, D.H. Olson, Atlas of Zeolites Framework Types, Structure Commission of the IZA, fifth ed., Elsevier, 2001.
[2] A. Alberti, G. Vezzalini, V. Tazzoli, Zeolites 1 (1981) 91–97.
[3] J.J. Pluth, J.V. Smith, Å. Kvick, Zeolites 5 (1985) 74–80.
[4] G. Gottardi, E. Galli, Natural Zeolites, Springer-Verlag, Heidelberg, 1985, p. 409.
[5] T. Armbruster, M.E. Gunter, D.L. Bish, in: D.W. Ming (Ed.), Reviews in Mineralogy and Geochemistry, 45, Mineralogical Society of America and Geochemical Society, Chantilly, Virginia, 2001, pp. 1–57.
[6] P. Feng, X. Bu, G.D. Stucky, Nature 388 (1997) 735–741.
[7] S. Neeraj, S. Natarajan, J. Phys. Chem. Solid. 62 (2001) 1499–1505.
[8] Y.X. Ke, G.F. He, J.M. Li, Y.G. Zhang, S.M. Lu, New J. Chem. 25 (2001) 1627–1630.
[9] Y.J. Lee, S.J. Kim, J.B. Parise, Microporous Mesoporous Mater. 34 (2000) 255–271.
[10] P. Feng, T. Zhang, X. Bu, J. Am. Chem. Soc. 123 (2001) 8608–8609.
[11] W.H. Taylor, C.A. Meek, W.W. Jackson, Z. Kristallogr. 84 (1933) 373–398.
[12] S.T. Amirov, I.R. Amiraslanov, B.T. Usubaliev, K.S. Mamedov, Azerb. Khim. Zh. 3 (1978) 120–127.
[13] G.D. Gatta, V. Kahlenberg, R. Kaindl, N. Rotiroti, P. Cappelletti, M. De' Gennaro, Am. Mineral. 95 (2010) 495–502.
[14] K. Ståhl, Å. Kivick, J.V. Smith, Acta Crystallogr. C 46 (1990) 1370–1373.
[15] L.P. Van Reeuwijk, Am. Mineral. 57 (1972) 499.
[16] K. Ståhl, R. Thomasson, J. Appl. Crystallogr. 25 (1992) 251–258.
[17] M. Giordani, M. Mattioli, M. Cangiotti, A. Fattori, M.F. Ottaviani, M. Betti, P. Ballirano, A. Pacella, D. Di Giuseppe, V. Scongnamiglio, M. Hanusckova, A. F. Gualtieri, Chemosphere 291 (2022), 133067.
[18] CrysAlisPro 171.42.58a, Rigaku Oxford Diffraction, 1995-2022.
[19] G.M. Sheldrick, Acta Crystallogr. A 64 (2008) 112–122.
[20] G.M. Sheldrick, Acta Crystallogr. C 71 (2015) 3–8.
[21] K. Momma, F. Izumi, J. Appl. Crystallogr. 44 (2011) 1272–1276.
[22] H.-W. Wang, D. Bish, Eur. J. Mineral 22 (2010) 271–284.
[23] D.L. Bish, H.-W. Wang, Philos. Mag. 90 (17) (2010) 2425–2441.
[24] K. Ståhl, R. Thomasson, Zeolites 14 (1994) 12–17.
[25] G. Cametti, R.M. Danisi, T. Armbruster, M. Nagashima, Microporous Mesoporous Mater. 208 (2015) 171–180.
[26] G.D. Gatta, Eur. J. Mineral 17 (2005) 411–421.
[27] P. Comodi, G.D. Gatta, P.F. Zanazzi, Eur. J. Mineral 14 (2002) 567–574.
[28] Y. Lee, J.A. Hriljac, A. Studer, T. Vogt, Phys. Chem. Miner. 31 (2004) 22–27.